

Photon GRID Radiation Therapy: A Physics and Dosimetry White Paper from the Radiosurgery Society (RSS) GRID/LATTICE, Microbeam and FLASH Radiotherapy Working Group

Authors: Zhang, Hualin, Wu, Xiaodong, Zhang, Xin, Chang, Sha X., Megooni, Ali, et al.

Source: Radiation Research, 194(6) : 665-677

Published By: Radiation Research Society

URL: <https://doi.org/10.1667/RADE-20-00047.1>

BioOne Complete (complete.BioOne.org) is a full-text database of 200 subscribed and open-access titles in the biological, ecological, and environmental sciences published by nonprofit societies, associations, museums, institutions, and presses.

Your use of this PDF, the BioOne Complete website, and all posted and associated content indicates your acceptance of BioOne's Terms of Use, available at www.bioone.org/terms-of-use.

Usage of BioOne Complete content is strictly limited to personal, educational, and non - commercial use. Commercial inquiries or rights and permissions requests should be directed to the individual publisher as copyright holder.

BioOne sees sustainable scholarly publishing as an inherently collaborative enterprise connecting authors, nonprofit publishers, academic institutions, research libraries, and research funders in the common goal of maximizing access to critical research.

Photon GRID Radiation Therapy: A Physics and Dosimetry White Paper from the Radiosurgery Society (RSS) GRID/LATTICE, Microbeam and FLASH Radiotherapy Working Group

Hualin Zhang,^{a,1} Xiaodong Wu,^b Xin Zhang,^c Sha X. Chang,^d Ali Megooni,^e Eric D. Donnelly,^a Mansoor M. Ahmed,^{f,2} Robert J. Griffin,^g James S. Welsh,^h Charles B. Simone, IIⁱ and Nina A. Mayr^j

^a Department of Radiation Oncology, Northwestern University Feinberg School of Medicine, Chicago, Illinois 60611; ^b Executive Medical Physics Associates and Biophysics Research Institute of America, Miami, Florida 33179; ^c Department of Radiation Oncology, Boston Medical Center, Boston, Massachusetts 02118; ^d Department of Radiation Oncology, University of North Carolina School of Medicine, Chapel Hill, North Carolina 27516; ^e Department of Radiation Therapy, Comprehensive Cancer Center of Nevada, Las Vegas, Nevada 89169; ^f Division of Cancer Treatment and Diagnosis, Rockville, Maryland 20892; ^g University of Arkansas for Medical Sciences, Department of Radiation Oncology, Little Rock, Arkansas; ^h Loyola University Chicago, Edward Hines Jr. VA Hospital, Stritch School of Medicine, Department of Radiation Oncology, Maywood, Illinois 60153; ⁱ New York Proton Center, Department of Radiation Oncology, New York, New York 10035; and ^j Department of Radiation Oncology, University of Washington Medical Center, Seattle, Washington 98195

Zhang, H., Wu, X., Zhang, X., Chang, S. X., Megooni, A., Donnelly, E. D., Ahmed, M. M., Griffin, R. J., Welsh, J. S., Simone, C. B. II and Mayr, N. A. Photon GRID Radiation Therapy: A Physics and Dosimetry White Paper from the Radiosurgery Society (RSS) GRID/LATTICE, Microbeam and FLASH Radiotherapy Working Group. *Radiat. Res.* 194, 665–677 (2020).

The limits of radiation tolerance, which often deter the use of large doses, have been a major challenge to the treatment of bulky primary and metastatic cancers. A novel technique using spatial modulation of megavoltage therapy beams, commonly referred to as spatially fractionated radiation therapy (SFRT) (e.g., GRID radiation therapy), which purposefully maintains a high degree of dose heterogeneity across the treated tumor volume, has shown promise in clinical studies as a method to improve treatment response of advanced, bulky tumors. Compared to conventional uniform-dose radiotherapy, the complexities of megavoltage GRID therapy include its highly heterogeneous dose distribution, very high prescription doses, and the overall lack of experience among physicists and clinicians. Since only a few centers have used GRID radiation therapy in the clinic, wide and effective use of this technique has been hindered. To date, the mechanisms underlying the observed high tumor response and low toxicity are still not well understood. To advance SFRT technology and plan-

ning, the Physics Working Group of the Radiosurgery Society (RSS) GRID/Lattice, Microbeam and Flash Radiotherapy Working Groups, was established after an RSS-NCI Workshop. One of the goals of the Physics Working Group was to develop consensus recommendations to standardize dose prescription, treatment planning approach, response modeling and dose reporting in GRID therapy. The objective of this report is to present the results of the Physics Working Group's consensus that includes recommendations on GRID therapy as an SFRT technology, field dosimetric properties, techniques for generating GRID fields, the GRID therapy planning methods, documentation metrics and clinical practice recommendations. Such understanding is essential for clinical patient care, effective comparisons of outcome results, and for the design of rigorous clinical trials in the area of SFRT. The results of well-conducted GRID radiation therapy studies have the potential to advance the clinical management of bulky and advanced tumors by providing improved treatment response, and to further develop our current radiobiology models and parameters of radiation therapy design. © 2020

by Radiation Research Society

INTRODUCTION

Megavoltage X-ray GRID therapy is a form of spatially fractionated radiation therapy (SFRT) that has been used successfully to manage patients with bulky tumors, which are often refractory to conventional radiation therapy and other cancer therapies (1, 2). GRID therapy employs an X-ray fluence in a spatially-fractionated irradiation pattern in the shape of a grid (grid pattern). This grid pattern is created by the use of a physical GRID block (3) or GRID collimator that contain arrays of apertures within a Cerrobend or brass block. Newer technologies also

¹ Address for correspondence: Department of Radiation Oncology, Northwestern University Feinberg School of Medicine, Northwestern Memorial Hospital, Chicago, IL 60611; email: hzhang@nm.org.

² This article reflects the scientific opinion for the RSS Working Group established after an RSS-NCI Workshop, August 2018. Members of the National Cancer Institute (NCI) participate in this group. This is the personal professional judgment of the member, Mansoor M. Ahmed and does not represent opinion, guidance, position statement or policy of the Radiation Research Program, Division of Cancer Treatment and Diagnosis, NCI, Department of Health and Human Services or U.S. government.

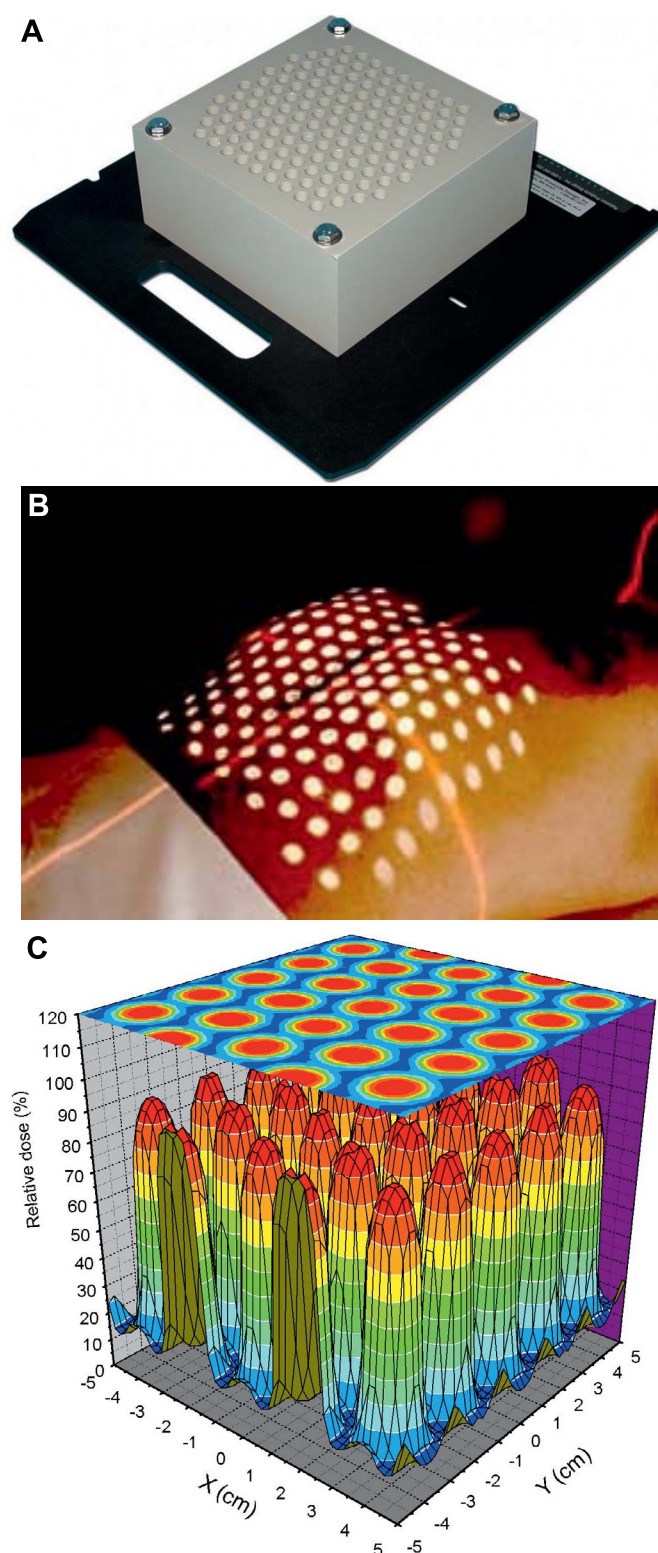


FIG. 1. The GRID block (High Dose Radiation GRID; Radiation Products Design) and field.

include grid pattern generation by a treatment planning system through a virtual block and entirely by multileaf collimator (MLC) modulation (4). A typical GRID collimator is shown in Fig. 1 and the resulting dose

distribution illustrated by the light field pattern on a patient's skin. GRID therapy is not new; GRID radiation fields were initially used to overcome the challenges of treating deep-seated tumors in the kilovoltage X-ray era before the 1950s (5). The technology has subsequently been adapted to megavoltage beams and the first clinical study using megavoltage GRID therapy was published in 1990 (1). Initially, GRID therapy showed success in reducing tumor size and inducing high rates of symptomatic response in very bulky, palliatively treated tumors in patients with metastatic cancer. Over the past 30 years, ample clinical evidence has accumulated for the high symptomatic and clinical response and minimal toxicity of GRID therapy in palliatively and definitively treated tumors with excessive bulk and/or therapy resistance (1, 6–16). More recently, SFRT has also been used as a boost or “priming” therapy to improve response to definitive or preoperative radiation in bulky, locally advanced curable tumors (1, 10–16). The mechanisms hypothesized to underpin the observed responses in GRID therapy, such as immunological, bystander and microvascular effects, continue to be an area of active research (17–19). The purpose of this article is to provide a clinical physics consensus and guidelines for technology selection, commissioning, quality assurance (QA), dose prescription, treatment planning and reporting for GRID therapy, and staff training. Based on the consensus, recommendations are made to standardize these physics and dosimetry processes for all GRID therapy plans to improve clinical treatments, facilitate the interpretation of clinical trial results and further aid the elucidation of translational biological parameters underpinning the effects of SFRT, based on a consistent and standardized approach to dosing, delivery and dose reporting of this unique and complex treatment approach.

MATERIALS AND METHODS

In view of the unique characteristics of SFRT, and the lack of widespread familiarity among medical physicists with the principles and intricacies of GRID therapy, the RSS GRID/Lattice, Microbeam and Flash Radiotherapy set of Working Groups established the Physics Working Group after an RSS-NCI Workshop in August 2018, to develop and provide recommendations, guidelines and procedures for GRID therapy as a special treatment modality that can be applied for clinical management and clinical trials. The recommendations were developed based on a comprehensive review of the physics and clinical literature. The consensus was specifically focused on the GRID component of treatment because ample guidelines exist for the conventional radiation therapy component that is often combined with GRID. Lattice therapy, a variant and a 3-dimensional (3D) configuration of SFRT with an array of high-dose regions generated by converging intensity-modulated beams or volumetric modulated arc therapy (VMAT), was felt to be beyond the scope of this article. Based on this review the Physics Working Group determined that there is an urgent need to provide an up-to-date review of GRID therapy and to develop and propose guidelines for GRID therapy technology selection, commissioning, dose calibration, dosimetric approaches, treatment planning and evaluation, treatment dose prescription and reporting, QA and staff training. The guidelines

development process included close collaboration with dosimetrists, radiobiology experts and radiation oncologists to ensure that basic science as well as the clinical perspective were brought into this clinical physics consensus work.

CLINICAL RESULTS REVIEW

Based on a phone survey with physicians and physicists in five radiation therapy centers in the U.S. that have used GRID therapy, at least 2,000 patients have been treated with this technique nationwide. While no data are available on the exact total number of patients who have received GRID therapy, the actual number of patients treated with GRID therapy could be significantly higher than the survey data above. Currently, at least one clinical trial of GRID therapy is ongoing on in the U.S. (20).

Several studies have evaluated the clinical efficacy of GRID therapy in a variety of settings. Mohiuddin *et al.* (10) reported that among 87 patients with bulky and therapy-refractory tumors of various histologies (sarcoma, squamous cancer, adenoma, melanoma and others) treated palliatively with GRID therapy, an overall palliative symptom response rate of 94% was achieved with doses greater than 15 Gy prescribed to the *dmax* depth in one fraction at 3–42 months of follow-up. With doses less than 15 Gy, the response was decreased to 62%. Response was higher when GRID therapy was followed by conventionally fractionated open-field uniform external-beam therapy (92%), compared to GRID therapy alone (86%). Furthermore, open-field external-beam radiation doses of 40 Gy or greater resulted in higher response than lower doses. Mohiuddin *et al.*'s study thereby provided foundational dose-response relationship data for GRID therapy and for the combination open-field uniform external beam radiation. It also demonstrated the need to combine GRID therapy with open-field uniform external beam radiation to improve the probability of clinical symptom response in advanced bulky palliatively treated tumors.

While the original GRID therapies were delivered using Cerrobend GRID blocks on non-digital accelerators (Fig. 1), MLCs on digital accelerators have enabled GRID fields with the added ability to shape the field to conform to the tumor volume and spare organs at risk (OARs). Several investigators have studied advanced treatment planning systems (TPS) to design virtual GRID blocks (21–23), where the function of the physical GRID block is achieved by software and multileaf collimators (Fig. 2), as well as the use of multiple beams and arc 3D treatment approaches. Lattice therapy, a variant of SFRT, employs non-coplanar focused beams or VMAT to generate an array of individual high-dose spherical vertices within the tumor while reducing the peripheral tumor dose (24). Furthermore, proton therapy centers have begun exploring proton beams in GRID therapy beam configurations employing pencil beam scanning (25, 26).

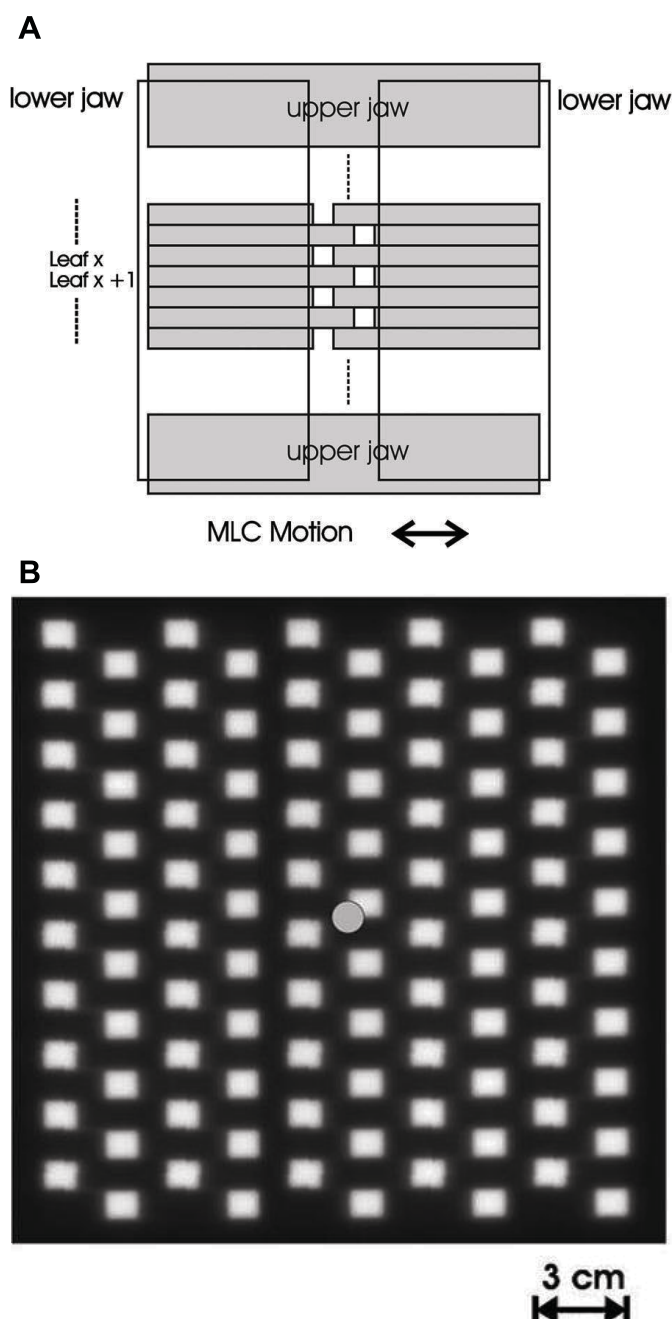


FIG. 2. The MLC-created GRID radiation field (4). MLCs also could be used to generate grid-like field. In this example, five separate MLC-shaped beams were used, and each defined two columns of the grid openings. The composite of the five beams gave rise to an effective “GRID” with the openings arranged in an alternating checkerboard pattern and open-to-close areal ratio of 1:3 (4).

While there is increasing interest among clinicians in the use of SFRT techniques to treat patients, there is no established clinical guidance to assist them in treatment planning and evaluation. In addition, as more GRID therapy techniques and planning methods become available, their complexity and variation increases significantly, making meaningful evaluation and comparison of

techniques challenging for both clinical care and for the development, analysis and reporting of clinical trials.

UNIQUE CONSIDERATIONS FOR PHOTON GRID THERAPY AND DOSIMETRY

The key technical, dosimetric and workflow parameters of GRID therapy include treatment prescription, non-uniform dose planning and evaluation (such as peak and valley dose ratio and equivalent uniform dose), delivery technique selection [3D-CRT, conformal arc, intensity-modulated radiation therapy (IMRT), TomoTherapy, VMAT and proton therapy], selection of energy corresponding to patient-specific GRID therapy target (shallow or deep-seated, size and shape of target volume, sparing or disregarding of the critical OARs, considering or disregarding the neutron and electron contamination, etc.), and treatment delivery time consideration with practical treatment times (as longer treatment times may cause patient motion and discomfort as well as slow workflow throughput).

Although some investigators have proposed methods to standardize the dose documentation (27), a consensus has not been established. In addition, GRID therapy has been used under diverse clinical regimens, ranging from one to several fractions of GRID therapy, followed by a standard several-week course of uniform radiation. Furthermore, these variable regimens have also been used in variable combinations with chemotherapy. Major ongoing questions focus on the dose criteria of GRID therapy, and whether and how the dose from GRID radiation should be added in the patients' conventionally fractionated radiation course, so as to establish consistency when treatment response end points are evaluated. It is anticipated that the more precise and standardized the implementation and reporting of the physical treatment parameters are in clinical GRID therapy trials, the more robust will be the resulting dose parameters and clinical outcome correlations.

EQUIPMENT, COMMISSIONING AND QUALITY ASSURANCE

Attention to technology implementation, commissioning and robust quality assurance processes is of critical importance for the establishing and maintaining a SFRT program, and should be tailored to the individual facility's capabilities and needs. The following procedures for commissioning the GRID collimator and treatment QA are recommended.

Water Phantom Measurements

Before the GRID collimator is used in clinic, a water phantom dosimetric study must be performed, since different linear accelerators may have different beam properties. All water phantom measurements can be

performed using a water scanning system. The water scanning system usually consists of a $48 \times 48 \times 48 \text{ cm}^3$ or similar size water tank, an electrometer, an ionization chamber and data acquisition/processing software. The GRID collimator is placed in the blocking tray slot of the linear accelerator. Data are acquired for 6-MV and 10-MV photon beams at 100 cm source-to-surface distance (SSD). Beam energies above 10 MV are not used to avoid neutron production. Depth ionization scans are obtained along the beam central axis under the central aperture of the grid for 5×5 , 10×10 , 15×15 and $20 \times 20 \text{ cm}^2$ collimator jaw settings. GRID output factors are measured at 1.5, 2 and 5 cm depth for $10 \times 10 \text{ cm}^2$ jaw setting. The scanning system is carefully aligned to maintain the ion chamber at the center of the beam profile at all depths. Depth doses are assumed to be directly obtainable from the normalized depth ionization profiles without any further consideration for loss of electronic equilibrium or energy spectrum changes. Cross-beam ionization profiles at 5×5 , 10×10 , 15×15 and $20 \times 20 \text{ cm}^2$ collimator jaw settings are respectively obtained in both the transverse and radial planes at a depth of 1.5 cm for 6-MV beam and at 2 cm for 10-MV beam. Cross-beam ionization profiles at the depth of 3, 5 and 10 cm are also measured. Because the grid apertures of commercially available GRID collimators are arranged in a hexagonal close-packed form, as further discussed in *Commercially available GRID collimators* in the section, *Treatment Planning for Spatially Fractionated (GRID) Radiation Therapy*, the transverse profiles cut the grid along a line joining opposite apertures of the central hexagon, whereas the radial profiles cut the grid along a line bisecting opposite sides of the central hexagon. Therefore, the spacing between the peaks and the heights of the peaks and valleys in the profiles are different for the two orthogonal scan directions. The transverse and radial dose profiles can be obtained directly from the normalized ionization profiles without any further consideration for loss of electronic equilibrium or energy spectrum changes. A detailed example of the water phantom measurements is given in the subsection, *Example of a Physical GRID Collimator Commissioning* and Table 1.

Film Dosimetry

EBT film (Eastman Kodak, Rochester, NY) has been widely used in radiotherapy applications, including IMRT quality assurance, and it has been shown to have a better dose-response range and improved linearity (28). In the past, EDR2 films (by the same company) were also used to measure GRID dose distribution at depths of interest (29). As a convenient tool, films can be utilized to obtain the dose output factor and dosimetric distributions at the tumor depth. Calibration curves should be obtained for each batch of film. With the film, beam profiles of the GRID field will be obtained in both the radial and transverse directions, as well as in a full 2D representation.

TABLE 1
Percentage Depth Doses for a 6-MV 10×10 cm² GRID Field and an Open Field (29)

Distance from water surface D (cm)	GRID field 10×10 CM ² (WATER TANK)	GRID field 10×10 CM ² (MONTE CARLO)	Open field 10×10 CM ² (WATER TANK)	Open field 10×10 cm ² (Monte Carlo)
0.0	45.5	45.0	45.0	44.3
0.5	70.1	83.6	75.1	74.8
1.0	96.2	94.9	95.7	96.4
1.5	100.0	100.0	100.0	100.0
2.0	98.3	98.6	99.4	99.1
2.5	95.7	94.7	97.6	97.0
3.0	93.4	94.8	95.7	95.1
3.5	90.5	90.8	93.6	92.9
4.0	88.3	89.3	91.4	90.8
4.5	85.4	84.7	89.4	88.6
5.0	83.5	83.5	87.3	86.7
5.5	80.9	80.4	85.2	84.5
6.0	77.7	77.2	83.1	82.4
6.5	76.7	73.9	81.1	80.4
7.0	74.7	74.7	79.3	78.2
7.5	72.4	72.8	77.2	76.2
8.0	70.0	70.5	75.2	74.2
8.5	68.0	69.1	73.3	72.5
9.0	66.2	66.2	71.5	70.6
9.5	64.4	63.8	69.6	68.8
10.0	62.8	62.2	67.8	66.9
10.5	60.7	59.4	66.1	65.1
11.0	59.3	58.2	64.3	63.4
11.5	57.1	55.2	62.6	61.7
12.0	54.9	55.7	60.9	60.0
12.5	54.1	51.4	59.4	58.2
13.0	52.3	51.5	57.8	56.7
13.5	50.8	51.1	56.2	55.3
14.0	48.5	47.8	54.6	53.8
14.5	47.9	45.8	53.3	52.1
15.0	46.4	44.8	51.8	50.7
15.5	44.9	42.5	50.5	49.4
16.0	43.5	41.2	49.2	48.2
16.5	41.7	41.2	47.9	46.9
17.0	39.9	40.5	46.6	45.5
17.5	39.4	38.0	45.3	44.3
18.0	38.8	36.8	44.0	43.0
18.5	37.7	36.6	42.8	41.9
19.0	35.6	36.2	41.6	40.7
19.5	36.1	33.7	40.5	39.7
20.0	34.1	33.3	39.4	38.5

Note. Gantry is at zero degree, distance is from the top water surface located at 100 cm source-to-surface distance (SSD) to downstream.

Monte Carlo Simulation

If possible, a Monte Carlo simulation can be performed to obtain dosimetric characteristics of the GRID field at different jaw settings and different tumor depths to complement experimental data, but the results must be experimentally validated. The next section provides a detailed example of Monte Carlo dosimetric characterization of a GRID collimator in detail.

Example of a Physical GRID Collimator Commissioning

This section describes the typical process of GRID collimator commissioning and serves as an example for clinical practice. This commissioning work was carried out

at the University of Kentucky prior to implementation of the first systematic GRID therapy program, and in its concept has been published elsewhere (29).

Water phantom scanning work. The water phantom measurements were performed according to the standard procedure described above in *Water Phantom Measurements* section, using the $48 \times 48 \times 48$ cm³ water tank, electrometer and two scanning ion-chambers set-up. A Wellhoeffler CC01 microionization chamber was used for all in-field measurements. The results are shown in Table 1. Measurements were performed using a commercial GRID collimator (High Dose Radiation GRID; Radiation Products Design, Albertville, MN). The 6-MV photon beam was set at 100 cm SSD of a Clinac 2100 EX linear accelerator

(Varian Oncology Systems, Palo Alto, CA). As per procedures, the depth ionization scans were acquired along the central axis under the central aperture of the grid for 5×5 , 10×10 , 15×15 and 20×20 cm² collimator jaw settings, and cross-beam ionization profiles were acquired in both the transverse and radial planes at a depth of 1.5 cm. The depth doses were assumed to be directly obtainable from the normalized depth ionization profiles without any further consideration for loss of electronic equilibrium or energy spectrum changes. The transverse and radial dose profiles were obtained directly from the normalized ionization profiles.

EDR2 film dosimetry. EDR2 film (Eastman Kodak) was irradiated in solid-water (Gammex RMI, Middleton, WI) slab phantoms to obtain cross-beam profiles. Films were irradiated at a depth of 1.5 cm using 6-MV photons from a Clinac 2100 EX linear accelerator (Varian Oncology Systems). Calibration curves were obtained for each batch of film. The film was processed at least 3 h postirradiation to minimize known time-dependent film sensitivity (15). All films were scanned using an Epson Expression 1680 flatbed scanner (Epson® America Inc., Long Beach, CA) and analyzed with Procheck version 2.7 (NMPE, Lynnwood, WA). Beam profiles of the GRID field were obtained in both the radial and transverse directions, as well as in a full 2D representation.

Monte Carlo simulation. A Monte Carlo N-particle Transport Code (MCNPX, version 2.5) (30) was used to calculate the doses in water at a depth of 1.5 cm. Results of the Monte Carlo simulation are given in Table 1. The code is the extension for particle types and energy ranges of MCNP (31). The photon interaction cross-section file used in this study was the DLC-200 library distributed by the Radiation Shielding Information Computing Center (RSICC). The MCNPX code considers photoelectric, coherent, Compton and pair production interactions. There are several tally types available in the MCNPX code for dose calculation. The *f8 tally calculates the difference between the energy carried into and out of the tally cell by particles. In this project, the *f8 tally type was used to determine the dose-rate distribution in the flat water phantom at the depth of interest, 1.5 cm, as well as the central axis percentage depth dose. A simplified source model (29), first described by DeMarco *et al.* (32) and Lewis *et al.* (33), was used. Although this design ignores the true photon phase space distribution, as pointed out by Siebers *et al.* (34), its effectiveness and accuracy have been demonstrated for flat phantoms when fine beam structure is not emphasized. However, this simplified model ignores the existence of electron contamination in photon beam. The cone-beam angle was chosen to allow a maximum field size of 40×40 cm² on the phantom surface at 100 cm SSD by collimators located 53 cm from the source. A spectrum representative of photon energies that exit the monitor ionization chamber was used. This spectrum was previously determined for a Varian 21 EX 6-MV photon beams by Spezi *et al.* (35) and validated by comparison to that obtained from

EGS4 code (36). The grid collimator was simulated as a 2D array of 19 conical apertures having with hole diameters of 0.60 cm on the top side and 0.85 cm on the lower side and a 7.5-cm length arranged within a Cerrobend block in the hexagonal pattern. All holes in the grid were divergent and roughly concordant with the beam tilt. The measurements have shown that this design produced the same output from all of the holes. The SSD for the phantom was set at 100 cm. An array of spherical, 1-mm-diameter tally cells, spaced at 2 mm center-to-center, was defined at depths ranging from 0.25 to 7 cm at 0.25-cm increments for simulating 2D dose at each layer. The dose distributions from all layers constituted a 3D dose distribution. The depth dose was obtained using 1-mm voxels with a 2-mm spacing arranged along the beam central axis. For each simulation, the low-energy cutoff was set at 10 keV and used a minimum of 5×10^8 histories. The statistical error of each tallied dose was found to be less than 4%.

Treatment Planning Dose Calculation

Treatment planning dose calculation must be commissioned for GRID therapy using the commissioning measurement data. The treatment planning system already commissioned for conventional radiation therapy may not be adequate for GRID therapy and must be validated using the GRID therapy experimental data before clinical use. Many modern Monte Carlo codes are available for radiotherapy beam simulation, and readers are encouraged to explore this topic (29, 37, 38). Importantly, all dose calculations, including the Monte Carlo simulation, must be validated by GRID commissioning through experimental work before clinical use, as exemplified in detail in the subsection, *Example of a Physical GRID Collimator Commissioning*.

GRID TREATMENT PRESCRIPTION

Although different GRID therapy prescription doses have been reported, most clinics use the prescription ranging from 10 to 20 Gy to the open dose spot. If the tumor is shallowly seated (<3 cm deep), it is recommended that the central hole maximum dose is set to be equal to the dose at depth of d_{max} and used as the prescription dose. If the GRID aperture size is very small, the maximum dose from the hole field may become sensitive to the size of the detector that is used experimentally or Monte Carlo simulation. In this scenario, the peak is very sharp, and one half of aperture physical size (half of aperture diameter) can be used to obtain average maximum dose at the depth of d_{max} . This has been proven effective since the field is divergent, and the projected fields are magnified at the treatment distance. This dose is also referred to as the nominal dose.

For deeply-seated tumors (>3 cm depth), it is recommended that the dose at the tumor center depth be used as the prescription dose. When a commercially available GRID

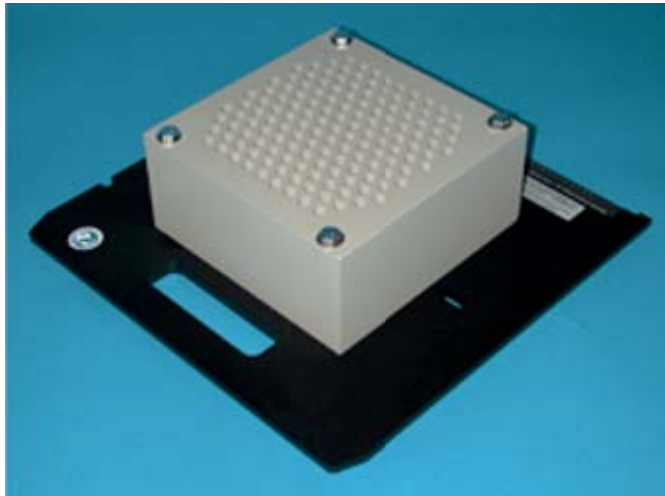


FIG. 3. Commercially available GRID collimator (High Dose Radiation Grid; Radiation Products Design).

collimator is used, the dose at the prescription depth onto the central axis of the central hole is defined as the prescription dose. The same definitions for dose prescription apply to the MLC-based GRID therapy, and the prescription point is on or near the beam's central axis, or near the field center.

TREATMENT PLANNING FOR SPATIALLY FRACTIONATED (GRID) RADIATION THERAPY

Commercially Available GRID Collimators

Most clinics use commercially available GRID collimators, currently available from two companies (High Dose Radiation Grid; Radiation Products Design; .decimal®, Sanford, FL). Early GRID therapy was generated by GRID blocks with a hexagonal array of apertures within a Cerrobend block. Preceding the development of MLCs, this GRID block did not allow MLC-based field shaping. The concept was then further developed into the currently used GRID collimators that allow both a grid pattern of irradiation and MLC-based field collimation. The original GRID collimator (manufactured by Radiation Products Design), consisted of a 7.5-cm thick Cerrobend block, perforated by a hexagonal pattern (Fig. 3) of circular divergent holes, and was designed to be mounted in the standard linear accelerator accessory mount 65.4 cm from the source (Varian 21 EX, Varian Oncology Systems, Palo Alto, CA). The GRID collimator configuration was subsequently advanced to a new design using brass as a construction material to reduce weight (.decimal). The diameter of the holes is 0.60 cm on the top side and 0.85 cm on the lower side, and the center-to-center separation of the holes on the block is 1.15 cm on the lower surface. With the original GRID collimator design, approximately one half of the tissues in the collimated areas were irradiated by the partially attenuated primary beam; the remainder were

shielded by the Cerrobend block. All holes in the GRID were divergent and roughly concordant with the beam tilt. For the commonly used, commercially available GRID collimators, the MU needed for delivering the prescribed nominal dose (i.e., 15 or 20 Gy) is calculated based on the output factor of the central hole usually near, or passing through, the beam's central axis. The approach is the same for the MLC-formed or jaw-formed GRID fields. Because when the commercially available GRID collimator is mounted, an MLC or jaw-pairs can be used to reduce the field size to create a preliminary conformal field adapted to the tumor size, the output factor (OUT_{dmax}) of the GRID field central hole at the depth of d_{max} will vary with the field size and must be measured. The MU is calculated according to:

$$MU = \frac{D_{nominal}(Gy)}{OUT_{dmax}(\frac{Gy}{MU})}. \quad (1)$$

For instance, if a GRID field has an output factor of 0.89 cGy/MU at the depth of d_{max} of GRID field central hole, we can calculate and know that 2,247 MUs will be needed for giving 20 Gy at the d_{max} depth of the GRID field (2,000 cGy/0.89 cGy/MU). If the machine dose rate is 600 cGy/min, the treatment will take 3.75 min.

The water tank measurements indicate that, although the percentage depth dose (PDD) curve has noticeably changed compared to the open field, when the GRID aperture size is approximately 1 cm, the depth of d_{max} remains the same for 10×10 cm² jaw size (3, 29). Thus, when we generate plans and perform the QAs, we can still use the d_{max} depths measured from the open field (Fig. 4). Table 1 provides an example of GRID field PDD that readers can use as a reference. While GRID beam data from various linacs are very similar if the energy and setting are kept constant, variations in the GRID collimator can alter the results. As we can see, the planning technique is very straightforward, and we are simply calculating and delivering the nominal prescription dose (e.g., 20 Gy) to the depth of d_{max} of the GRID beamlet field. Because each beamlet may be slightly different, we choose the central hole passing through the beam's central axis as the standard for MU calculation.

However, the depth of the tumor center may be variable, and the treating physician may decide to prescribe the dose to a depth (d) other than d_{max} . In addition, if two opposed GRID fields are used (39), then the PDD curves would be entirely different. If this is the case, then the physicist must measure or calculate the GRID field output factor at d . Again, the calculated output factor needs to be experimentally verified. If the output factor of the GRID field at the depth d is OUT_d , then,

$$MU = \frac{D_{nominal}(Gy)}{OUT_d(\frac{Gy}{MU})}. \quad (2)$$

Figure 5 shows the peaks and valleys of doses of the GRID field. These peaks and valleys are spatially populated with

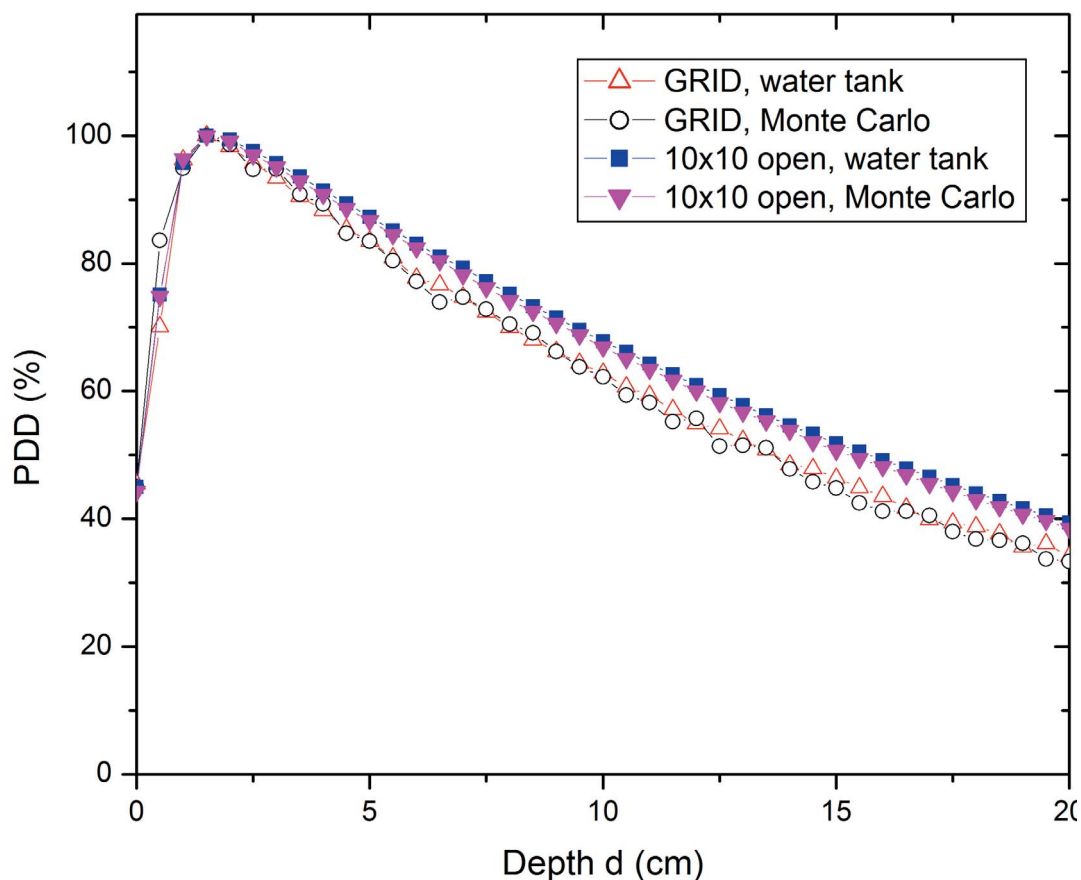


FIG. 4. Percentage depth-dose curves of a 10×10 cm² open field and a 10×10 cm² GRID field. The PDD of the GRID field is measured by water tank and calculated using the Monte Carlo technique (29).

the designed pattern, which produces the SFRT. In GRID therapy, another important dosimetric parameter is the valley/peak (in some studies, presented as peak/valley) dose ratio, VPDR or R , described as:

$$R = \frac{\text{Valley dose}}{\text{Peak dose}}. \quad (3)$$

The VPDRs are variable (Fig. 6) and dependent on the GRID collimator configuration, depth and energy. For example, in one type of commercially available GRID (the diameter of the holes was 0.60 cm on the top side and 0.85 cm on the lower side, and the center-to-center separation on the block was 1.15 cm on the lower surface), it was found that when depth was increased from 1.5 cm to 5 cm, the dose ratio between peak and valley decreased from 5.9 to 5.1 (40), or VPDR increased from 0.17 to 0.20.

It should be noted that, because block collimator-based GRID therapy is largely performed with commercially available GRID collimators, most physics studies and clinical data are based on the hexagonal pattern, 1 cm aperture diameter and 1.5 cm center-to-center distance design of these collimators. Because different dose heterogeneities would be produced with different GRID collimator designs, it is reasonable to consider that

collimators with different aperture sizes and patterns might provide different dosimetric and tissue effects. The role of GRID collimators of different sizes, patterns and hole center-to-center distance have not been systematically explored. Future studies will be needed to provide more comprehensive characterization and a clearer understanding of the dosimetric and biological effects of GRID collimator design.

Planning Approach for MLC-Generated GRID Dose Distributions

Using modern MLCs and advanced TPS software, a GRID-like field and dose distribution can be created and delivered. Although the GRID apertures are made and adjusted in the TPS, because each beamlet (hole) is very small and its diameter may only range from 0.5 to 1.5 cm, the dose calculation from the TPS may not be accurate, mainly due to the fact that small-field dosimetry requires special attention (41). Therefore, its calculation accuracy must be commissioned beforehand, or the plan can be made through experimental measurement.

One approach recommended by the Physics Working Group for the planning is to place a Gafchromic™ film at the depth of the tumor center in solid-water slabs with

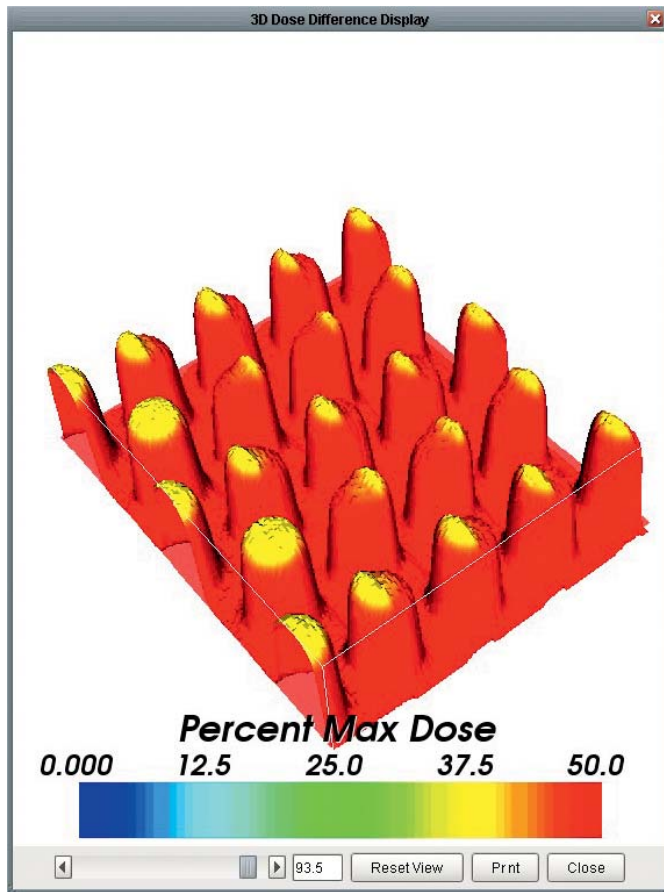


FIG. 5. The dose distribution at the d_{max} depth measured using film dosimetry (29).

enough backscattering, measure the dose at the central beamlet hot spot, then derive an output factor at that depth for the central beamlet hot spot by comparison with the film measurement result of the reference open field and film dose calibration curve; then calculate the total MU needed for delivering the prescription dose by dividing the prescription dose by the measured output factor. The output factors for other beamlet hot spot also must be verified, to ensure that the variation of output factors of the GRID beamlet hot spot across the target depth is within 5%.

What are the Useful Dosage Parameters of GRID Therapy?

Because the dose delivered by GRID therapy is highly non-uniform, the nominal dose (i.e., the dose delivered at the dose profile peak) likely does not fully represent the dose-response relationship for tumor control and cell kill achieved by GRID therapy. The equivalent uniform dose (EUD) can be employed to describe the GRID dose and calculate dose-tumor control parameters achieved by GRID therapy for the tumor volume.

It should be noted that there are several different approaches to estimate the EUDs of a non-uniform radiation field. Niemierko explored the EUD in the non-uniform

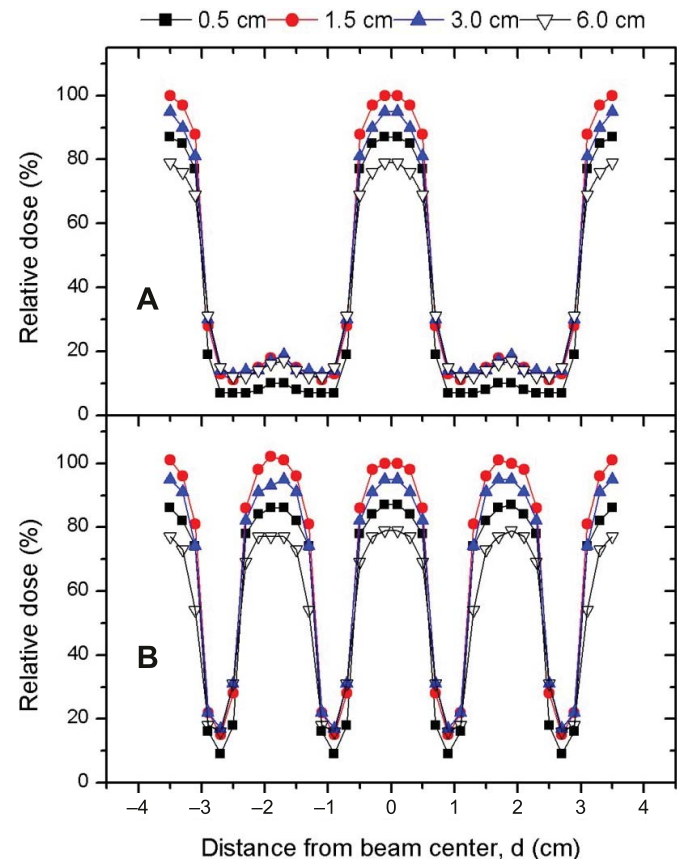


FIG. 6. Radial and transverse dose profiles of GRID therapy in a flat water phantom at 0.5, 1.5, 3.0 and 6 cm depths for a 6-MV beam. The doses were normalized to a 10×10 cm² open field at 1.5-cm depth, and 100 cGy was applied to the open field as a standard. Panels A and B: In plane and cross plane, respectively (40).

spatial distribution of dose in 1997, in which he introduced an equation where the EUD is calculated by adjusting the reference dose survival fraction in a given volume to the various local doses (42). The equation is as follows:

$$EUD = D_{ref} \times \frac{\ln \left\{ \frac{\sum_{i=1}^N \Delta V_i \times \rho_i \times (SF_2)^{\frac{D_i}{D_{ref}}}}{\sum_{i=1}^N \Delta V_i \times \rho_i} \right\}}{\ln(SF_2)}. \quad (4)$$

D_{ref} is a reference dose of 2 Gy, SF_2 is a reference survival fraction of the specific clonogen when treated with D_{ref} , D_i is the local dose and ΔV_i is the local volume corresponding to D_i . ρ_i is the local clonogen density.

In addition, applying the modified-linear-quadratic (MLQ) model, we can calculate the average surviving fraction of GRID therapy, and then an EUD can also be derived (40). The MLQ model instead of LQ model is preferable because the GRID therapy uses a nominal dose as high as 20 Gy, and consequently a significant volume of the tumor will receive doses of more than 10 Gy. In this high-dose range the LQ model tends to underestimate the cell

survival, as its radiosensitivities are obtained from the low-dose range for estimating the survival fraction (43–45).

A study comparing the EUDs calculated by Niemierko's model with the MLQ model demonstrated that the MLQ-based EUD is approximately 5% lower than that derived from Niemierko's equation (46). Because the MLQ model corrects the overkilling predicted by the LQ model and Niemierko's equation, we suggest that the EUD formalism proposed by Zhang *et al.* (40), described in detail below, be used to obtain the EUD of GRID therapy. Equation (5) is the MLQ model:

$$SF_i = \exp(-\alpha \times D_i - \beta * G(\lambda \times T + \delta \times D_i) \times D_i^2), \quad (5)$$

where SF_i is the survival fraction at the dose D_i , α and β are radiosensitivity parameters of the cell, $G(\lambda T) = \frac{2(\lambda T + e^{-\lambda T} - 1)}{(\lambda T)^2}$, λ is the repair rate ($T_{1/2} = \frac{\ln 2}{\lambda}$), $T_{1/2}$ is cell doubling time and T is the delivery time of the treatment.

The average survival fraction \overline{SF} was calculated with Eq. (6) using the MLQ parameters listed in Table 2 (46), breast cancer, for example.

$$\overline{SF} = \frac{\sum_{i=1}^{i=N} SF_i \times f_i}{100} \quad \sum_{i=1}^{i=N} f_i = 100. \quad (6)$$

f_i is the fraction of target volume receiving dose D_i . The average survival fraction was then utilized to solve MLQ Eq. (7) for deriving the equivalent uniform dose (EUD), namely by solving the following equation for EUD:

$$\exp(-\beta \times G(\lambda \times T + \delta \times (EUD)) \times (EUD)^2 - \alpha \times (EUD)) = \overline{SF}. \quad (7)$$

For a 3D tumor treated with the GRID therapy, an approximation equation was given elsewhere (27), shown here as Eq. (8):

$$EUD = 2.47 + 0.089 \times D_{nominal} \quad (D_{nominal} \geq 5\text{Gy}). \quad (8)$$

Figure 7 shows the relationship between the EUD and nominal dose for 3D tumors.

In addition, because the underlying reasons that GRID therapy induces potential dose-heterogeneity-dependent biological effects remain to be explored, it is essential to

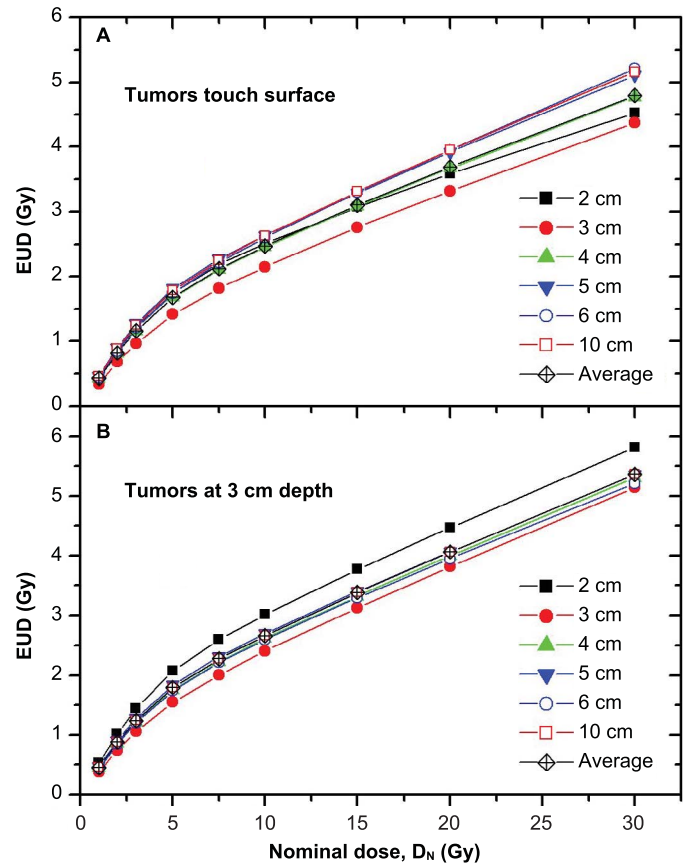


FIG. 7. The equivalent uniform doses (EUDs) of tumors of different sizes in single-fraction GRID therapy calculated using the MLQ model (40).

document dosimetric heterogeneity parameters in each treatment plan in a standardized fashion, so that potential correlations between the clinical outcomes and these parameters can be studied. The Physics Working Group recommends that dose covering 90%, 50%, 20%, 10% and 5% be documented along with other parameters, as outlined in Table 3.

How Well are Normal Cells Spared by Commercially Available GRID Collimators?

Similar biological modeling considerations apply to normal tissue effects of GRID therapy. The average

TABLE 2
MLQ Parameters of Breast Cancer Cell Lines (C1 and C2) and Normal Tissues (N1, N2 and N3)

	Breast cancer cell		Normal tissue		
	C1	C2	N1	N2	N3
α (Gy^{-1})	0.3	0.2	0.366	0.211	0.108
β (Gy^{-2})	0.03	0.052	0.118	0.068	0.035
α/β (Gy)	10	3.846	3.102	3.103	3.086
$T_{1/2}$ (h)	1	1	1	1	1
λ (h^{-1})	0.693	0.693	0.693	0.693	0.693
δ (Gy^{-1})	0.15	0.15	0.15	0.15	0.15

TABLE 3

Summary of recommended GRID commissioning approaches, beam data and GRID plan dosimetric metrics	
GRID commissioning	
Water tank measurement	
Film dosimetry	
Monte Carlo simulation	
GRID field beam data	
Percentage depth dose (PDD) at the central hole for 10 × 10 cm ² jaw setting	
GRID output factor at 1.5 cm, 2 cm and 5 cm depth for 10 × 10 cm ² jaw setting	
Transverse and radial plane dose profiles at 1.5 cm, 2 cm, 3 cm, 5 cm and 10 cm depth for 5 × 5, 10 × 10, 15 × 15 and 20 × 20 cm ² jaw settings	
Dosimetric metrics of GRID plan	
Prescription dose (D _p , in Gy)	
Equivalent uniform doses (EUD, in Gy) for tumor and normal tissues	
Output factor (OUT _d) at prescription depth (d) (in Gy/MU)	
Dose covering 90% of target (D90, in Gy)	
Dose covering 50% of target (D50, in Gy)	
Dose covering 20% of target (D20, in Gy)	
Dose covering 10% of target (D10, in Gy)	
Dose covering 5% of target (D5, in Gy)	
Mean dose of target (D _{mean})	
Valley/peak dose ratio (VPDR) ^a	
D90/D10 VPDR	
Peak width (defined at 50% of the max peak dose)	
Peak-to-peak distance	
Peak dose	
Valley dose	

^a The term “peak/valley dose ratio (PVDR)” is also in use.

surviving fraction of normal tissue in a GRID field $\overline{SF}_N(\text{Grid})$ was calculated using the same methodology as was used for the cancer cell line, but with the normal cell MLQ parameters (Table 2). The ratio between the value $\overline{SF}_N(\text{Grid})$ and the surviving fraction of normal cells using the EUD, i.e., $\overline{SF}_N(\text{EUD})$, will derive definitions with respect to the therapeutic ratio (TR) of GRID therapy according to:

$$TR = \frac{\overline{SF}_N(\text{grid})}{\overline{SF}_N(\text{EUD})}. \quad (9)$$

Because it is assumed that the GRID field and open field with the same EUD will achieve the same cancer cell-killing rate, a therapeutic advantage on normal tissue sparing by the GRID field is implied if TR is greater than 1, as the GRID therapy has spared more normal tissue. However, if the TR is less than 1, for the same cancer cell-killing rate (i.e., same tumor control), more normal cell death in the GRID field is implied, and uniform dose radiotherapy would be preferable over SFRT for the patient.

CONCLUSION AND DISCUSSION

We propose that the following recommendations be considered in the clinical use of GRID therapy for

dosimetric parameters and planning strategy for GRID collimator.

1. GRID therapy dose should be documented not only by the nominal dose at d_{max} , or at the prescription depth of the central axis of the central hole, but also by the EUD. Because the EUD slightly depends on the α/β ratios, the EUDs in treating all cancers can be approximated using Eq. (8) for hypofractionation (40).
2. The dose heterogeneity parameters describing VPDR, EUD and the dose D90, through D5 (Table 3) should all be documented.
3. The ratio of D_{valley}/D_{peak} , D90/D10 should be calculated and documented. The single point peak dose and single point valley dose may misrepresent the spatial fractionation in GRID therapy. Therefore, we suggest that a ratio of D90/D10 be used to replace the D_{valley}/D_{peak} ratio.
4. The specific GRID therapy dosing regimen should be tailored based on the clinical experience with its tumor-specific response and safety outcomes (1, 10, 13, 16, 27, 47).
5. GRID therapy should be followed by open-field external beam therapy to further control the disease in cases when durable tumor control is the goal. This is supported by both theoretical modeling and clinical outcomes indicating that SFRT can increase treatment response; however, because the EUD is only a fraction of the nominal dose, SFRT alone is not sufficient to provide tumor control (27).

The Physics Working Group further notes that these GRID therapy guidelines may have to be tailored based on the presumed treatment goals, such as debulking large tumors, sensitizing bulky tumors, changing tumor physiology or microenvironment, and possibly improving tumor immune response. In addition, further refinements of these consensus guidelines will likely be needed in the future based on emerging information in the rapidly progressing field of SFRT.

Received: February 20, 2020; accepted: September 18, 2020; published online: October 19, 2020

REFERENCES

1. Mohiuddin M, Curtis DL, Grizos WT, Komarnicky L. Palliative treatment of advanced cancer using multiple nonconfluent pencil beam radiation. A pilot study. *Cancer* 1990; 66:114–8.
2. Yan W, Khan MK, Wu X, Simone CB, 2nd, Fan J, Gressen E, et al. Spatially fractionated radiation therapy: History, present and the future. *Clin Transl Radiat Oncol* 2020; 20:30–8.
3. Meigooni AS, Dou K, Meigooni NJ, Gnaster M, Awan S, Dini S, et al. Dosimetric characteristics of a newly designed grid block for megavoltage photon radiation and its therapeutic advantage using a linear quadratic model. *Med Phys* 2006; 33:3165–73.
4. Ha JK, Zhang G, Naqvi SA, Regine WF, Yu CX. Feasibility of delivering grid therapy using a multileaf collimator. *Med Phys* 2006; 33:76–82.
5. Marks H. A new approach to the roentgen therapy of cancer with the use of a GRID. *J Mt Sinai Hosp N Y* 1950; 17:46–8.

6. Liberson, F. The value of a multi-perforated screen in deep X-ray therapy. *Radiology* 1933; 20:10.
7. Puri DR, Chou W, Lee N. Intensity-modulated radiation therapy in head and neck cancers: dosimetric advantages and update of clinical results. *Am J Clin Oncol* 2005; 28:415–23.
8. Marks H. Clinical experience with irradiation through a grid. *Radiology* 1952; 58:338–42.
9. Miller RC, Wilson KG, Feola JM, Urano M, Yaes RJ, McLaughlin P, et al. Megavoltage grid total body irradiation of C3Hf/SED mice. *Strahlenther Onkol* 1992; 168:423–6.
10. Mohiuddin M, Fujita M, Regine WF, Megooni AS, Ibbott GS, Ahmed MM. High-dose spatially-fractionated radiation (GRID): a new paradigm in the management of advanced cancers. *Int J Radiat Oncol Biol Phys* 1999; 45:721–7.
11. Sathishkumar S, Dey S, Meigooni AS, Regine WF, Kudrimoti MS, Ahmed MM, et al. The impact of TNF-alpha induction on therapeutic efficacy following high dose spatially fractionated (GRID) radiation. *Technol Cancer Res Treat* 2002; 1:141–7.
12. Sathishkumar S, Boyanovsky B, Karakashian AA, Rozenova K, Giltiay NV, Kudrimoti M, et al. Elevated sphingomyelinase activity and ceramide concentration in serum of patients undergoing high dose spatially fractionated radiation treatment: implications for endothelial apoptosis. *Cancer Biol Ther* 2005; 4:979–86.
13. Huhn JL, Regine WF, Valentino JP, Meigooni AS, Kudrimoti M, Mohiuddin M. Spatially fractionated GRID radiation treatment of advanced neck disease associated with head and neck cancer. *Technol Cancer Res Treat* 2006; 5:607–12.
14. Reiff JE, Huq MS, Mohiuddin M, Suntharalingam N. Dosimetric properties of megavoltage grid therapy. *Int J Radiat Oncol Biol Phys* 1995; 33:937–42.
15. Trapp JV, Warrington AP, Partridge M, Philips A, Glees J, Tait D, et al. Measurement of the three-dimensional distribution of radiation dose in grid therapy. *Phys Med Biol* 2004; 49:N317–23.
16. Penagaricano JA, Moros EG, Ratanatharathorn V, Yan Y, Corry P. Evaluation of spatially fractionated radiotherapy (GRID) and definitive chemoradiotherapy with curative intent for locally advanced squamous cell carcinoma of the head and neck: initial response rates and toxicity. *Int J Radiat Oncol Biol Phys* 2010; 76:1369–75.
17. Mackonis EC, Suchowerska N, Zhang M, Ebert M, McKenzie DR, Jackson M. Cellular response to modulated radiation fields. *Phys Med Biol* 2007; 52:5469–82.
18. Asur RS, Sharma S, Chang CW, Penagaricano J, Kommuru IM, Moros EG, et al. Spatially fractionated radiation induces cytotoxicity and changes in gene expression in bystander and radiation adjacent murine carcinoma cells. *Radiat Res* 2012; 177:751–65.
19. Asur R, Butterworth KT, Penagaricano JA, Prise KM, Griffin RJ. High dose bystander effects in spatially fractionated radiation therapy. *Cancer Lett* 2015; 356:52–7.
20. Penagaricano J. Phase I clinical trial of GRID therapy in pediatric osteosarcoma of the extremity. NIH/U.S. National Library of Medicine: Bethesda, MD; 2017. (<https://bit.ly/2G3ZAHc>)
21. Costlow HN, Zhang H, Das IJ. A treatment planning approach to spatially fractionated megavoltage grid therapy for bulky lung cancer. *Med Dosim* 2014; 39:218–26.
22. Jin JY, Zhao B, Kaminski JM, Wen N, Huang Y, Vender J, et al. A MLC-based inversely optimized 3D spatially fractionated grid radiotherapy technique. *Radiother Oncol* 2015; 117:483–6.
23. Stathakis S, Esquivel C, Gutierrez AN, Shi C, Papanikolaou N. Dosimetric evaluation of multi-pattern spatially fractionated radiation therapy using a multi-leaf collimator and collapsed cone convolution superposition dose calculation algorithm. *Appl Radiat Isot* 2009; 67:1939–44.
24. Blanco Suarez JM, Amendola BE, Perez N, Amendola M, Wu X. The use of Lattice radiation therapy (LRT) in the treatment of bulky tumors: A case report of a large metastatic mixed mullerian ovarian tumor. *Cureus*. 2015; 7:e389.
25. Henry T, Ureba A, Valdman A, Siegbahn A. Proton grid therapy: A proof-of-concept study. *Technol Cancer Res Treat* 2017; 16:749–57.
26. Henry T, Bassler N, Ureba A, Tsubouchi T, Valdman A, Siegbahn A. Development of an interlaced-crossfiring geometry for proton grid therapy. *Acta Oncol* 2017; 56:1437–43.
27. Zhang H, Wang JZ, Mayr N, Kong X, Yuan J, Gupta N, et al. Fractionated grid therapy in treating cervical cancers: conventional fractionation or hypofractionation? *Int J Radiat Oncol Biol Phys* 2008; 70:280–8.
28. Khachonkham S, Dreindl R, Heilemann G, Lechner W, Fuchs H, Palmans H, et al. Characteristic of EBT-XD and EBT3 radiochromic film dosimetry for photon and proton beams. *Phys Med Biol* 2018; 63:065007.
29. Zhang H, Johnson EL, Zwicker RD. Dosimetric validation of the MCNPX Monte Carlo simulation for radiobiologic studies of megavoltage grid radiotherapy. *Int J Radiat Oncol Biol Phys* 2006; 66:1576–83.
30. Hendricks JS, McKinney GW, Waters LS, Roberts TL, Egendorf HW, Finch JP, et al. MCNPX, version 2.5.e, LA-UR-04-0569. Los Alamos, NM: Los Alamos National Laboratory; 2004.
31. collection Rcc. Monte Carlo N-particle transport code system. Los Alamos, NM: Los Alamos National Laboratory; 2000.
32. DeMarco JJ, Solberg TD, Smathers JB. A CT-based Monte Carlo simulation tool for dosimetry planning and analysis. *Med Phys* 1998; 25:1–11.
33. Lewis RD, Ryde SJ, Hancock DA, Evans CJ. An MCNP-based model of a linear accelerator x-ray beam. *Phys Med Biol* 1999; 44:1219–30.
34. Siebers JV, Keall PJ, Libby B, Mohan R. Comparison of EGS4 and MCNP4b Monte Carlo codes for generation of photon phase space distributions for a Varian 2100C. *Phys Med Biol* 1999; 44:3009–26.
35. Spezi E, Lewis DG, Smith CW. Monte Carlo simulation and dosimetric verification of radiotherapy beam modifiers. *Phys Med Biol* 2001; 46:3007–29.
36. Nelson WR HH, Roger DWO. The EGS4 code system Stanford Linear Accelerator Center. Internal Report SLAC 265. Stanford, CA: Stanford University; 1985.
37. Martinez-Rovira I, Puxeu-Vaque J, Prezado Y. Dose evaluation of Grid therapy using a 6 MV flattening filter-free (FFF) photon beam: A Monte Carlo study. *Med Phys* 2017; 44:5378–83.
38. Chegeni N, Karimi AH, Jabbari I, Arvandi S. Photoneutron dose estimation in GRID therapy using an anthropomorphic phantom: A Monte Carlo study. *J Med Signals Sens* 2018; 8:175–83.
39. Meigooni AS, Gnaster M, Dou K, Johnson EL, Meigooni NJ, Kudrimoti M. Dosimetric evaluation of parallel opposed spatially fractionated radiation therapy of deep-seated bulky tumors. *Med Phys* 2007; 34:599–603.
40. Zhang H, Zhong H, Barth RF, Cao M, Das IJ. Impact of dose size in single fraction spatially fractionated (grid) radiotherapy for melanoma. *Med Phys* 2014; 41:021727.
41. Palmans H, Andreo P, Huq MS, Seuntjens J, Christaki KE, Meghizifene A. Dosimetry of small static fields used in external photon beam radiotherapy: Summary of TRS-483, the IAEA-AAPM International Code of Practice for reference and relative dose determination. *Med Phys* 2018; 45:e1123–45.
42. Niemierko A. Reporting and analyzing dose distributions: a concept of equivalent uniform dose. *Med Phys* 1997; 24:103–10.
43. Brenner DJ. The linear-quadratic model is an appropriate methodology for determining isoeffective doses at large doses per fraction. *Semin Radiat Oncol* 2008; 18:234–9.
44. Chapman JD, Gillespie CJ. The power of radiation biophysics—let's use it. *Int J Radiat Oncol Biol Phys* 2012; 84:309–11.

45. Kirkpatrick JP, Meyer JJ, Marks LB. The linear-quadratic model is inappropriate to model high dose per fraction effects in radiosurgery. *Semin Radiat Oncol* 2008; 18:240–3.
46. Saleh Y, Zhang H. Technical note: Dosimetric impact of spherical applicator size in intrabeam IORT for treating unicentric breast cancer lesions. *Med Phys* 2017; 44:6706–14.
47. Neuner G, Mohiuddin MM, Vander Walde N, Golubeva O, Ha J, Yu CX, et al. High-dose spatially fractionated GRID radiation therapy (SFGRT): a comparison of treatment outcomes with Cerrobend vs. MLC SFGRT. *Int J Radiat Oncol Biol Phys* 2012; 82:1642–9.